28. S. Jurac *et al.*, *Geophys. Res. Lett.* **29**, 2172 (2002).
29. R. E. Johnson *et al.*, *Icarus* **77**, 311 (1989).
30. D. E. Shemansky, P. Matheson, D. T. Hall, H.-Y. Hu, T. M. Tripp, *Nature* **363**, 329 (1993).
31. H. Balsiger *et al.*, *Nature* **321**, 330 (1986).
32. S. Jurac, R. E. Johnson, J. D. Richardson, C. Paranicas, *Planet. Space Sci.* **49**, 319 (2001).
33. D. A. Gurnett *et al.*, *Science* **307**, 1255 (2005).
34. L. W. Esposito *et al.*, in *Saturn*, T. Gehrels, M. S. Edwards, Eds. (Univ. of Arizona Press, Tucson, AZ, 1984), pp. 463–545.
35. This identification was made without time-of-flight (TOF) spectra because at this time, the IMS TOF system was not operating at full voltage and so was out of calibration. Further analysis of the spectra will allow us to positively identify the ion species.
36. W.-I. Ip, *Icarus* **115**, 295 (1995).
37. R. E. Johnson, T. I. Quickenden, P. D. Cooper, A. J. McKinley, C. Freeman, *Astrobiology* **3**, 823 (2003).
38. R. E. Johnson *et al.*, in *Jupiter: The Planet, Satellites, and Magnetosphere*, F. Bagenal, T. Dowling, W. B. McKinnon, Eds. (Cambridge Univ. Press, Cambridge, 2004), pp. 485–512.
39. M. Shi *et al.*, *J. Geophys. Res.* **100**, 26387 (1995).
40. R. E. Johnson, T. I. Quickenden, *J. Geophys. Res.* **102**, 10985 (1997).
41. The CAPS instrument and investigation represent the culmination of 16 years of effort by a team of 170 engineers and scientists at 15 institutions in 6 countries. We wish to thank all team members for their contributions and dedication to the CAPS and Cassini effort. Data reduction and analysis in the United States is supported by NASA/Jet Propulsion Laboratory under contract 1243218 with the Southwest Research Institute. Work at Los Alamos was performed under the auspices of the U.S. Department of Energy. We also wish to thank national funding agencies in Finland, France, Hungary, Norway, and the UK Particle Physics and Astronomy Research Council for their support.

7 October 2004; accepted 10 December 2004
10.1126/science.1106151

REPORT

Cassini Magnetometer Observations During Saturn Orbit Insertion

M. K. Dougherty,[1]* N. Achilleos,[1] N. Andre,[2] C. S. Arridge,[1] A. Balogh,[1] C. Bertucci,[1] M. E. Burton,[3] S. W. H. Cowley,[4] G. Erdos,[5] G. Giampieri,[1] K.-H. Glassmeier,[6] K. K. Khurana,[7] J. Leisner,[7] F. M. Neubauer,[8] C. T. Russell,[7] E. J. Smith,[3] D. J. Southwood,[9] B. T. Tsurutani[3]

Cassini's successful orbit insertion has provided the first examination of Saturn's magnetosphere in 23 years, revealing a dynamic plasma and magnetic environment on short and long time scales. There has been no noticeable change in the internal magnetic field, either in its strength or its near-alignment with the rotation axis. However, the external magnetic field is different compared with past spacecraft observations. The current sheet within the magnetosphere is thinner and more extended, and we observed small diamagnetic cavities and ion cyclotron waves of types that were not reported before.

The first in situ observations from Saturn's magnetosphere in 23 years were obtained during Cassini's Saturn orbit insertion on 30 June 2004. The magnetometer instrument (*1*) (MAG) obtained data on upstream waves, bow shock, magnetosheath, magnetopause, magnetospheric currents, and waves, as well as the planetary magnetic field. These data are consistent with measurements made on earlier missions, provide more detail of some parameters such as the planetary magnetic field, including its possible secular variation, and reveal some features in the external field not previously reported.

The solar wind controls the size of the magnetosphere and the dynamics of its outer reaches. Because the solar wind speed is supersonic, the deflection of the solar wind occurs via a standing bow shock that compresses and heats the solar wind, forming the magnetosheath. The inner edge of the magnetosheath, the magnetopause, marks the outer boundary of the region controlled by the planetary magnetic field. Saturn's bow shock is of intrinsic interest because it is expected to be much stronger than that of Earth. The magnetopause is important because it controls the coupling of the solar wind flow to the magnetosphere, principally, we expect, through the process known as reconnection (*2*). The locations of both boundaries are determined by the dynamic pressure of the solar wind and the combined plasma and magnetic pressure of the magnetosphere.

The boundaries were observed to be very dynamic. We measured a total of 17 bow shock and 7 magnetopause crossings (Fig. 1) on the inbound and outbound passages. Bow shock crossings were identified by abrupt increases in the magnetic field magnitude where the solar wind was compressed and decelerated. As Cassini approached Saturn near 08:00 local time (LT), it crossed the bow shock on seven separate occasions, starting at 09:45 universal time (UT) on 27 June 2004 at a distance of $49.15R_S$ [$1\ R_S = 60{,}268$ km (*3*)]. The last inbound bow shock crossing occurred at 05:38:30 UT on 28 June 2004 at a distance of $40.5R_S$. At least 10 crossings of the bow shock were observed on the outbound leg in the magnetometer data, with the earliest bow shock crossing observed on 7 July 2004 at a radial distance range of $56R_S$ and the final bow shock crossing occurring on 14 July 2004 at $85R_S$. Saturn's bow shock is expected to be a strong quasi-perpendicular shock. A large overshoot in the magnetic field magnitude is a consistent feature of the shock crossings and is a typical feature of supercritical planetary bow shocks (*4*). These observations afford us the opportunity to study bow shocks at high Mach numbers, which are rarely observed on Earth. Indeed, the Mach number can be inferred from the amplitude of the overshoot $\delta B/B_0$ (*5*). The average value for the bow shocks observed is ~1.5, consistent with a fast magnetosonic Mach number as high as 8.

On the Saturnian side of the bow shock lies the magnetosheath, where the magnetic field is very turbulent and dominated by wave activity. The entrance into the magnetosphere was preceded by multiple crossings of the magnetopause on 28 June and 29 June 2004. On the outbound pass, the spacecraft exited the magnetosphere near 05:00 LT. The first excursions into the inner magnetosheath were characterized by the presence of mirror mode structures. The multiple crossings of these plasma boundaries reveal the dynamic character of Saturn's outer magnetosphere in response to variations in the solar wind ram pressure.

Before the Cassini arrival at Saturn, there had been three previous flybys: Pioneer 11 (*6*) and Voyager 1 and 2 (*7*, *8*). The spatial coverage of these flybys was limited, with the inbound trajectories all being in the noon sector and outbound Pioneer 11 and Voyager 1

[1]Blackett Laboratory, Imperial College London, SW7 2AZ, UK. [2]CESR, 31028 Toulouse, France. [3]Jet Propulsion Laboratory, California Institute of Technology, Pasadena, CA 91109, USA. [4]Department of Physics and Astronomy, Leicester University, Leicester, LE1 7RH, UK. [5]KFKI Research Institute for Particle and Nuclear Physics, H-1525 Budapest, Hungary. [6]Technische Universitat Braunschweig, D-38106 Braunschweig, Germany. [7]University of California Los Angeles Institute of Geophysics and Planetary Physics, Los Angeles, CA 90024, USA. [8]Institute for Geophysics and Meterology, Köln University, 50923 Köln, Germany. [9]European Space Agency, 75738 Paris, France.

*To whom correspondence should be addressed. E-mail: m.dougherty@imperial.ac.uk

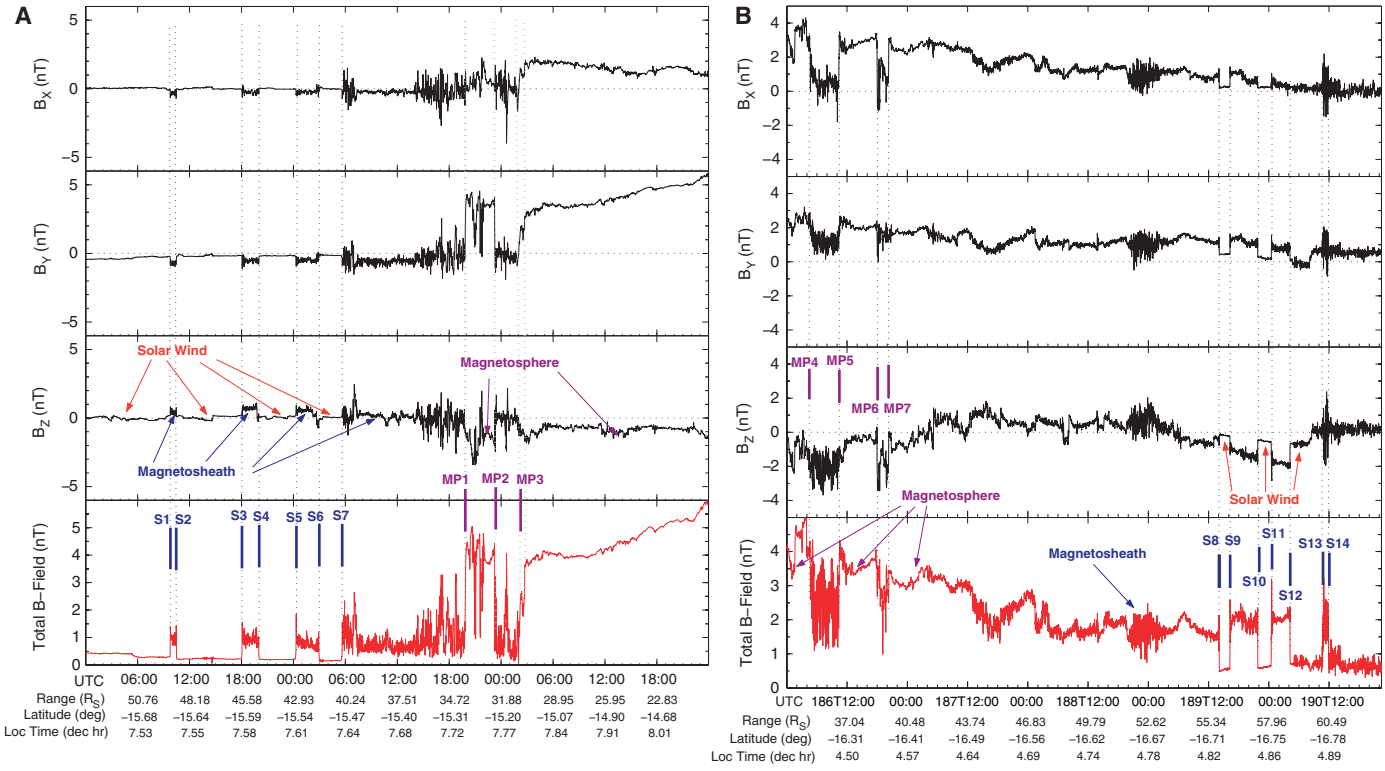

Fig. 1. (**A**) The magnetic field (*B*) between 27 and 29 June 2004 as the spacecraft approached Saturn. The top three sections show the three components of the field, with the magnitude depicted in the bottom section in KSM coordinates (*24*). Multiple bow shock (S1, S2, ...) and magnetopause (MP1, MP2, ...) crossings are indicated by vertical lines and labels. Information detailing the radial distance, latitude, and local time of the spacecraft with respect to Saturn are given. Time is given in universal time coordinated (UTC). (**B**) The magnetic field between 4 and 8 July 2004 on the outbound passage after Saturn orbit insertion.

exiting in the dawn meridian (Fig. 2). The inbound Cassini trajectory occurred at an earlier local time, and its outbound passage was similar to that of Voyager 2, exiting at high southern latitudes. A measure of the variability in the position of the different plasma boundaries can be assessed by comparing the locations of the Cassini crossings with their nominal position as deduced from the previous observations (*9*, *10*). The Cassini inbound crossings occurred further from Saturn than their average expected locations, revealing an expanded magnetosphere at the time of the inbound encounter (Fig. 2) with the first magnetopause crossing occurring a day earlier than expected. The state of the magnetosphere during the outbound part of the orbit was very different. The magnetopause and bow shock crossings were located inside their respective average surfaces, in agreement with a magnetosphere in a compressed regime. This regime is consistent with predictions (*11*) from upstream magnetic observations during the approach to Saturn. The entry into the magnetosphere was identified from the draping of the magnetic field, which is compatible with a dipole. In addition, an expansion of the magnetosphere occurred during the outbound passage of Cassini, with the magnetopause moving back out over the spacecraft and with the last bow shock occurring close to the expected nominal distance at $85R_S$.

In situ measurements of the internal magnetic field at Saturn have been obtained from the three previous flyby missions. The Cassini mission as an orbiter will provide a much more complete three-dimensional sampling of the magnetic field over the next 4 years. Until more complete measurements of the Saturnian magnetosphere are obtained during future orbits, the insertion observations (Fig. 3) can essentially be treated as a single flyby. In particular, for the inversion of the internal field we used only data within $8R_S$ and assumed an axisymmetric field configuration up to degree 3. External terms were also included by adding an axisymmetric ring current whose presence was revealed by analysis of previous data. Previous analyses led to the SPV and Z3 models (*12*, *13*), which included terms corresponding to a uniform external field in a source-free region. However, we have found that such a uniform field is not adequate for describing the field in and near the ring current, and therefore we have used the more realistic Connerney model adapted to Saturn (*14*, *15*).

Precise knowledge of the gain and pointing of the magnetometer is important for the accurate inversion of the measurements to obtain the internal magnetic field. We performed extensive ground calibrations before launch, checked the calibrations during the Earth flyby, and monitored the calibrations since launch with the magnetic field produced by coils both remote from and near the sensors. We estimate the uncertainty is presently 0.1% in gain and 0.1° in pointing. The magnetic field data were analyzed by using a standard singular value decomposition of the inversion matrix. Only zonal terms up to degree 3 are included in addition to the four disk parameters (namely, total current, inner and outer radii, and thickness). The internal field coefficients are shown (Table 1) alongside those from past models.

The quantity $g_{20}/(2g_{10})$, where g_{20} is the quadrupole moment and g_{10} the dipole moment, can be interpreted as a northward displacement of the dipole by $0.037R_S$. The comparable results for the SPV, Z3, and GD (*15*) models are $0.037R_S$, $0.038R_S$, and $0.037R_S$, respectively. The implication is that the magnetic and rotational equators do not coincide. However, the relatively large octupole moment cannot be explained by this offset. After accounting for the uncertainties associated with the estimated parameters, we were not able to determine any secular change in the internal field zonal coefficients. Also, we noticed that the azimuthal field component was barely visible near closest approach, which confirms the near-axial symmetry of the field. Although we have not considered the azimuthal component in our analysis because of the limited spatial sampling of the insertion trajectory, a previous study (*15*) has revealed the likely presence of a small azimuthal field

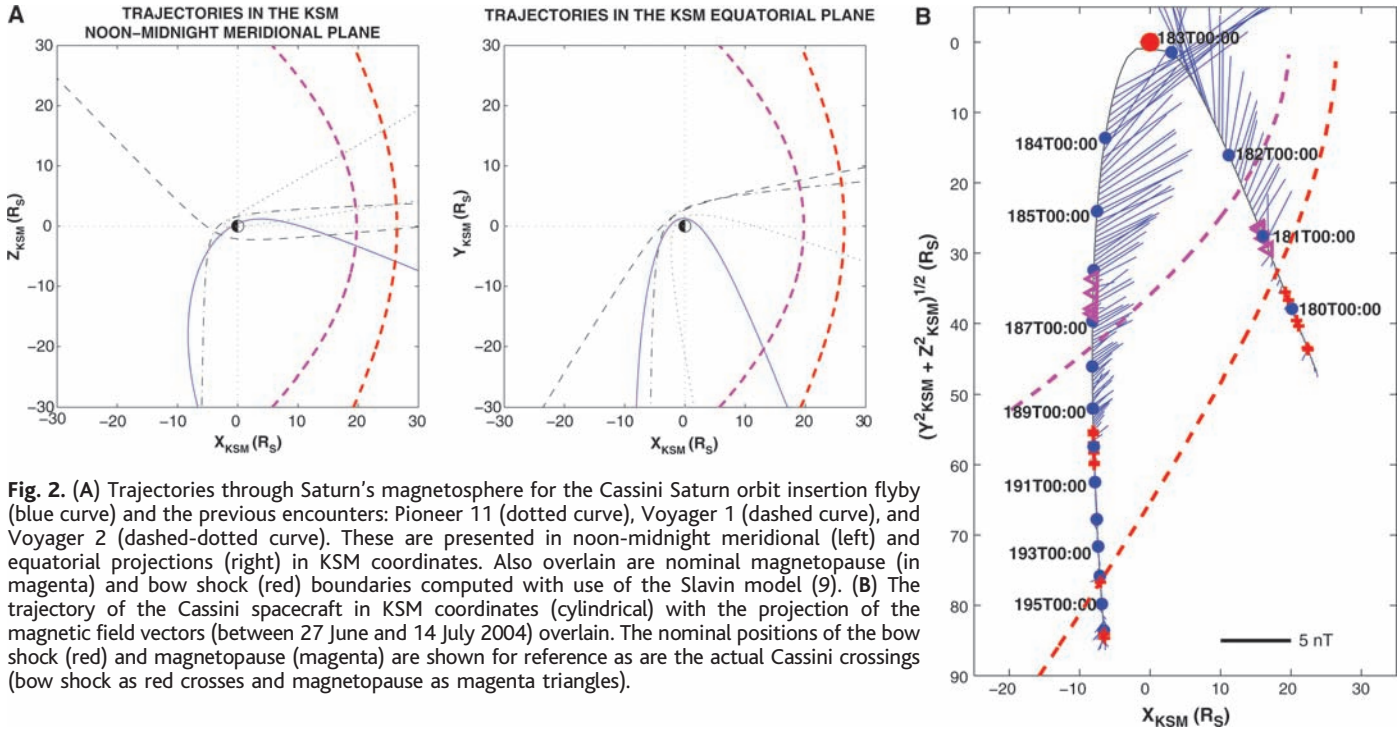

Fig. 2. (**A**) Trajectories through Saturn's magnetosphere for the Cassini Saturn orbit insertion flyby (blue curve) and the previous encounters: Pioneer 11 (dotted curve), Voyager 1 (dashed curve), and Voyager 2 (dashed-dotted curve). These are presented in noon-midnight meridional (left) and equatorial projections (right) in KSM coordinates. Also overlain are nominal magnetopause (in magenta) and bow shock (red) boundaries computed with use of the Slavin model (*9*). (**B**) The trajectory of the Cassini spacecraft in KSM coordinates (cylindrical) with the projection of the magnetic field vectors (between 27 June and 14 July 2004) overlain. The nominal positions of the bow shock (red) and magnetopause (magenta) are shown for reference as are the actual Cassini crossings (bow shock as red crosses and magnetopause as magenta triangles).

of internal origin, in accordance with theoretical constraints.

In the inner magnetosphere, the largest contribution to the external field was from the ring current, whose magnitude was as large as ~20 nT at the point where Cassini crossed the inner boundary of the disk ($r \sim 6R_S$). The estimated inner radius and current density of the disk are in very good agreement with our previous estimates; however, there are indications that the disk is thinner (half-thickness < $2R_S$) as well as more elongated (outer radius > $20R_S$) than in the past.

As in the case of the Earth and Jupiter, the magnetic field at Saturn is generated by three different current systems: in the core, in the magnetospheric plasma, and from the solar wind interaction with the planetary magnetic field. Subtracting the planetary magnetic field model allows us to examine the contribution of the various currents flowing inside the magnetosphere and on its boundaries. This differenced field ($\Delta\mathbf{B} = \mathbf{B}_{obs} - \mathbf{B}_{int}$) shown at radial distances greater than $4R_S$ can be seen in Fig. 4 in the black trace. Overlain on this figure are two different models of the external field in Saturn's magnetosphere. The blue trace is the best fit Connerney disk as described above, and the red trace is a new global magnetospheric model that models the external field, i.e., considering the internal field to be a fixed, known quantity.

In this global model, we retain the Connerney current disk to model the equatorial azimuthal current and used parameters obtained from the Voyager 1 flyby. The model also includes fields to represent the effect of magnetopause currents, which are modeled by the source-surface method (*16*) used in the Tsyganenko models of the terrestrial magnetosphere (*17*–*19*). We shield the magnetic field so that it is tangential to the magnetopause boundary at all points over that surface, which is represented by a prolate hemi-ellipsoid (*20*) for the nose region and a cylinder for the tail. The field due to the shielding of the dipole is represented with use of cylindrical harmonics and that due to the shielding of the disk with use of Cartesian harmonics. These representations allow the model to have an analytical dependence on the tilt angle between the dipole axis and the solar wind flow and on the solar wind dynamic pressure. The magnetopause stand-off distance, a function of the dynamic pressure, was set to be consistent with the location of the final inbound magnetopause crossing.

The global model does not fit the observed data well, and the current disk model suggests that the current disk field has changed compared with that of the Voyager 1 epoch. The magnitude of the azimuthal field in the outer magnetosphere caused by magnetopause currents is larger than that estimated from the model. This has also been seen in the previous flyby data sets (*21*) and may hint at further dynamical processes. At present, the model does not include a magnetotail current, which means we are underestimating the field in the tail region. Neither model accurately accounts for both the inbound and outbound observations simultaneously. This feature of the Saturnian magnetosphere has been noted in modeling studies and indicates an equatorial current disk that has local time structure and asymmetry. However, the compression of the magnetosphere during the Cassini flyby probably also altered the equatorial current distribution.

When Cassini was immersed within the plasma sheet, changes in the magnetic field

Table 1. Zonal harmonics from Saturn orbit insertion compared with past models (*25*). All coefficients are in reference to R_S = 60, 268 km. The first three models are axially symmetric up to degree 3; the fourth one includes also nonaxial terms up to the same degree.

Multipole term	Cassini	SPV	Z3	GD
g_{10}	21,084	21,225	21,248	21,232
g_{20}	1544	1566	1613	1563
g_{30}	2150	2332	2683	2821

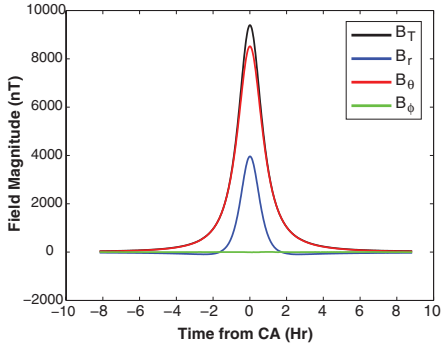

Fig. 3. The fluxgate magnetometer data from the closest approach (CA) period, with the three components and magnetic field magnitude shown.

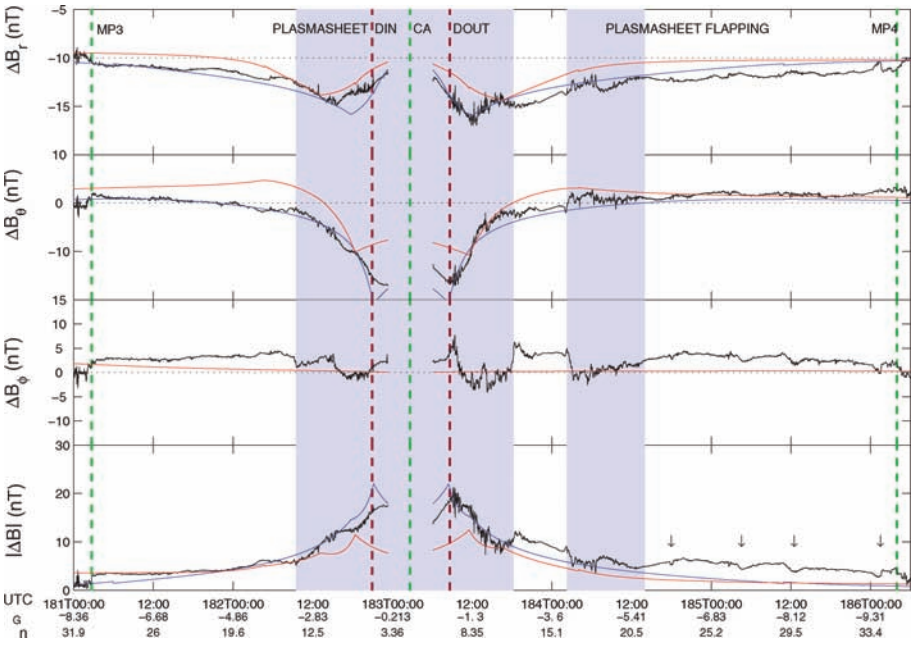

Fig. 4. Differenced field (black) in spherical polar coordinates obtained by subtracting the planetary field, as derived by the inversion of the Saturn orbit insertion data. This field represents the effect of magnetospheric current systems, and two models of this external field are overlaid. In blue is the best fit Connerney current disc (*14*) to the data, and in red is a new global model of Saturn's magnetospheric field. The last magnetopause crossing inbound and the first outbound crossing and perikron are indicated by vertical green dashed lines. The vertical crimson lines marked DIN and DOUT are crossings of Dione's L-shell inbound and outbound, respectively. The arrows indicate a quasi-periodic signature, which may also be plasma sheet–related. Shaded regions indicate where Cassini was immersed in the plasma sheet. Distance from the equatorial plane (z_{KG}) and range (r) are given in units of Saturn radii.

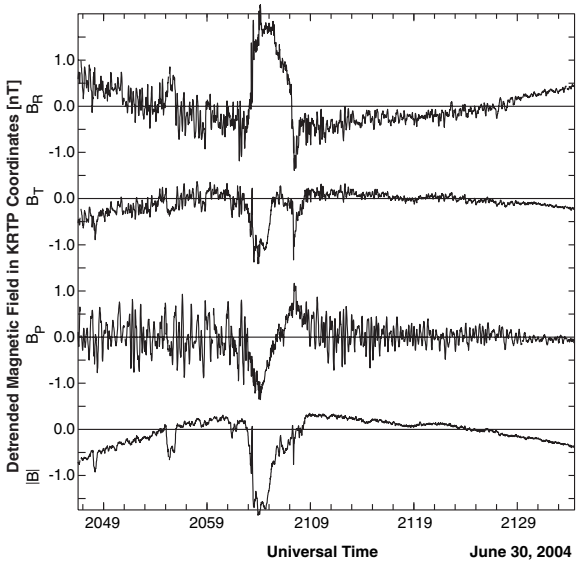

Fig. 5. Magnetic field strength through the largest and last diamagnetic depression seen on the inbound trajectory. Data have been detrended and is in KRTP, spherical polar Saturn centered coordinates, when R is radial array from Saturn, P is azimuthal, and T is meridional.

configuration occurred with an enhanced level of small-scale magnetic fluctuations. Outside of these regions, the Cassini spacecraft was located in the outer higher-latitude magnetosphere, a region with less plasma that is similar to the lobe regions of the Earth's magnetosphere. The plasma sheet crossings occurred at planetocentric distances of $15R_S$ inbound and $12R_S$ outbound and are associated with sharp transitions in the azimuthal field. The observed field fluctuations reveal a dynamic region associated with plasma sources, transport processes, and related wave generation. Closer to the planet the field is more dominated by the internal source. Outbound from about $16R_S$ and coincident with the Titan far encounter, the spacecraft may have again crossed the plasma sheet at high latitude, possibly caused by a dynamic solar wind–driven motion of the sheet. The field at these latitudes and distances is also tail-like, with a more stretched-out configuration.

On both the inbound and outbound legs of the pass, near but inside the orbit of Dione at $6.27R_S$, MAG encountered diamagnetic depressions in which some of the magnetic pressure was replaced by increased plasma pressure. On each leg the innermost depression was the largest. Such diamagnetic cavities were not reported for the Voyager and Pioneer flybys.

The largest of the depressions occurred at 21:05 UT on 30 June 2004 at a radial distance of $5.93R_S$, a local time of 09:45 LT, and a latitude of –9.5° (Fig. 5). Dione was at 15:08 LT. The maximum depth of the magnetic depression in the 95-nT background field was produced by a plasma with an energy density of 500 eV cm^{-3}. If produced by 1 keV electrons, a plasma density of about 0.5 electrons cm^{-3} would be required. On the outbound leg at 08:02 UT, $5.5R_S$, 01:53 LT, and –9° latitude, a similar depression was seen in a 115-nT background field corresponding to a plasma energy density of 300 eV cm^{-3}. If this is the outer boundary of a cold plasma torus, we would expect that the source of the cold ions would be the E ring and the hot electrons outside the cold torus region would be produced close to the ionosphere, where the field-aligned current system needed to enforce corotation of the plasma closes. Surrounding the two largest depressed field regions were relatively strong waves polarized in the direction transverse to the magnetic field. There was essentially no compressional component above the noise level of the instrument. Pioneer 11 (*22*) also saw transverse waves but beyond the orbit of Dione. The transverse Cassini waves are accompanied by a narrow band of left-hand cyclotron waves propagating very close to the direction of the magnetic field at the H_2O^+ gyro-frequency. Although seen on both sides of the depressions and on both legs, this narrow band of ion cyclotron waves makes very little contribution to the total wave power. The water group ion cyclotron waves are presumably associated with ion pickup from the E ring, but we do not have an obvious source for the strong linear transverse waves that surround the cavity. These are associated with the cavities because their amplitudes decrease with distance from the cavities.

At greater distances from the planet, the ratio of depressed to enhanced flux tubes increased until the field strength appeared to be continually depressed. The phenomenon in the Jovian magnetosphere that most nearly resembles these diamagnetic depressions is at the outer edge of the Io torus, at the boundary between the cold dense torus plasma and hotter magnetospheric plasma where flux tube interchange appears to take place (*23*). Alternatively this region may be where corotation of the magnetospheric plasma can no longer

be maintained by the ionosphere. The resulting slippage in the ionosphere heats the ionospheric electrons, producing high beta conditions along the entire flux tube.

Quite distinct from the waves surrounding the cavities was a 100-min-long burst of ion cyclotron waves (from 06:10 to 07:50 UT on 30 June 2004) unlike any seen on Voyager and Pioneer that appeared 5 hours after the Cassini engine stopped firing. These waves were limited to the frequency band expected for the singly ionized products of the engine exhaust H_2O, N_2, CO, and CO_2. We do not expect these waves to be present (except for H_2O^+ that may be associated with the icy satellites' environments) in the natural plasma. We note that Cassini's engine deposited over 850 kg of fuel in the Saturnian magnetosphere and, as it ionized and traversed the magnetosphere, it would produce a cloud of ions with energy predominantly transverse to the magnetic field, that is, a ring beam. The energy of these pickup ions at the locations where the waves were seen is comparable to that of the pickup ions in the Io torus. This may be the first detection of artificially induced plasma waves in a magnetosphere other than that of Earth.

References and Notes

1. M. K. Dougherty *et al.*, *Space Sci. Rev.* **114**, 331 (2004).
2. J. W. Dungey, *Phys. Rev. Lett.* **6**, 47 (1961).
3. International Astronomical Union standard definition of the Saturn equatorial body radius.
4. C. T. Russell, M. M. Hoppe, W. A. Livesey, *Nature* **296**, 45 (1982).
5. The ratio $\delta B/B0$ is the enhancement of the overshoot magnetic field normalized by the magnetosheath field strength away from the overshoot.
6. E. J. Smith *et al.*, *J. Geophys. Res.* **85**, 5655 (1980).
7. N. F. Ness *et al.*, *Science* **212**, 211 (1981).
8. N. F. Ness *et al.*, *Science* **215**, 558 (1982).
9. J. A. Slavin, E. J. Smith, P. Gazis, J. Mihalov, *Geophys. Res. Lett.* **10**, 9 (1983).
10. J. A. Slavin, E. J. Smith, J. Spreiter, S. Stahara, *J. Geophys. Res.* **90**, 6275 (1985).
11. C. M. Jackman *et al.*, *J. Geophys. Res.* **109**, A11203 (2004).
12. L. Davis, E. J. Smith, *J. Geophys. Res.* **95**, 15257 (1990).
13. M. H. Acuna, J. E. P. Connerney, N. F. Ness, *J. Geophys. Res.* **88**, 8771 (1983).
14. J. E. P. Connerney, M. H. Acuna, N. F. Ness, *J. Geophys. Res.* **88**, 8779 (1983).
15. G. Giampieri, M. K. Dougherty, *Geophys. Res. Lett.* **31**, 16701 (2004).
16. M. Schultz, M. C. McNab, *Geophys. Res. Lett.* **14**, 182 (1987).
17. N. A. Tsyganenko, *Planet. Space Sci.* **37**, 5 (1989).
18. N. A. Tsyganenko, *J. Geophys. Res.* **100**, 5599 (1995).
19. N. A. Tsyganenko, *J. Geophys. Res.* **107**, SMP12-1 (2002).
20. The dayside of the magnetopause is approximately ellipsoidal, but this is not the case in the tail, which is nearly circular in cross section. To accurately approximate the shape of the magnetopause, the tailward half of an ellipsoid is replaced with a cylinder; thus, the boundary is a composite surface composed of a hemi-ellipsoid and a cylinder. The join between these two surfaces is at the semi-minor axis of the prolate ellipsoid (nose portion).
21. E. J. Bunce, S. W. H. Cowley, J. A. Wild, *Ann. Geophys.* **21**, 1709 (2003).
22. E. J. Smith, B. T. Tsurutani, *J. Geophys. Res.* **88**, 7831 (1983).
23. C. T. Russell *et al.*, *Adv. Space Res.* **26**, 1489 (2000).
24. The KSM (Kronocentric Solar Magnetospheric) coordinate system has Saturn at the origin, with the $+X$ axis directed toward the Sun; Z defined such that Saturn's rotation and magnetic axis lies in the XZ plane (with $+Z$ pointing close to northward), and Y lying in Saturn's rotational and magnetic equatorial plane.
25. The reference for the SPV model is (*13*); for the Z3 model, (*14*); and the GD model, (*15*).
26. We wish to acknowledge the Cassini Project and operations team from the Jet Propulsion Laboratory, as well as the many people at our home institutions for their design, engineering, and software support over many years on behalf of this investigation. The contributions to the MAG team have been supported by the Particle Physics and Astronomy Research Council in the UK, Deutsches Zentrum für Luft-und Raumfahrt in Germany, and NASA in the U.S.

6 October 2004; accepted 7 December 2004
10.1126/science.1106098

REPORT

Dynamics of Saturn's Magnetosphere from MIMI During Cassini's Orbital Insertion

S. M. Krimigis,[1]* D. G. Mitchell,[1] D. C. Hamilton,[2] N. Krupp,[3] S. Livi,[1] E. C. Roelof,[1] J. Dandouras,[4] T. P. Armstrong,[5] B. H. Mauk,[1] C. Paranicas,[1] P. C. Brandt,[1] S. Bolton,[6] A. F. Cheng,[1] T. Choo,[1] G. Gloeckler,[2] J. Hayes,[1] K. C. Hsieh,[7] W.-H. Ip,[8] S. Jaskulek,[1] E. P. Keath,[1] E. Kirsch,[3] M. Kusterer,[1] A. Lagg,[3] L. J. Lanzerotti,[9,10] D. LaVallee,[1] J. Manweiler,[5] R. W. McEntire,[1] W. Rasmuss,[5] J. Saur,[1] F. S. Turner,[1] D. J. Williams,[1] J. Woch[3]

The Magnetospheric Imaging Instrument (MIMI) onboard the Cassini spacecraft observed the saturnian magnetosphere from January 2004 until Saturn orbit insertion (SOI) on 1 July 2004. The MIMI sensors observed frequent energetic particle activity in interplanetary space for several months before SOI. When the imaging sensor was switched to its energetic neutral atom (ENA) operating mode on 20 February 2004, at $\sim 10^3$ times Saturn's radius R_S (0.43 astronomical units), a weak but persistent signal was observed from the magnetosphere. About 10 days before SOI, the magnetosphere exhibited a day-night asymmetry that varied with an ~11-hour periodicity. Once Cassini entered the magnetosphere, in situ measurements showed high concentrations of H^+, H_2^+, O^+, OH^+, and H_2O^+ and low concentrations of N^+. The radial dependence of ion intensity profiles implies neutral gas densities sufficient to produce high loss rates of trapped ions from the middle and inner magnetosphere. ENA imaging has revealed a radiation belt that resides inward of the D ring and is probably the result of double charge exchange between the main radiation belt and the upper layers of Saturn's exosphere.

The magnetosphere of Saturn was discovered by Pioneer 11 in 1979 (*1*, *2*) and was investigated in detail by Voyager 1 in 1980 (*3*) and Voyager 2 in 1981 (*4*). The primary science objectives of MIMI (*5*) are to determine the global configuration and dynamics of hot plasma in the magnetosphere of Saturn through energetic neutral particle imaging of the ring current, radiation belts, and neutral clouds; to study the sources of plasmas and energetic ions through in situ measurements of energetic ion composition, spectra, charge state, and angular distribution; to search for, monitor, and analyze magnetospheric spatial and time variations; to determine through imaging and composition studies the magnetosphere-satellite interactions at Saturn; to understand the formation of clouds of neutral hydrogen, nitrogen, and water products; and to study Titan's comet-like interaction with Saturn's magnetosphere and the solar wind. The MIMI instrument (*5*) comprises three sensors that measure particles in specific energy ranges: (i) the Ion and Neutral Camera (INCA), which measures ion and

[1]Applied Physics Laboratory, Johns Hopkins University, Laurel, MD 20723, USA. [2]Department of Physics, University of Maryland, College Park, MD 20742, USA. [3]Max-Planck-Institut für Sonnensystemforschung, D-37191 Lindau, Germany. [4]Centre D'Etude Spatiale Des Rayonnements, F-31028 Toulouse, France. [5]Fundamental Technologies Inc., Lawrence, KS 66049, USA. [6]Jet Propulsion Laboratory, Pasadena, CA 91109, USA. [7]Department of Physics, University of Arizona, Tucson, AZ 85721, USA. [8]Graduate Institute of Astronomy, National Central University, Jhongli City, Republic of China. [9]Bell Laboratories, Murray Hill, NJ 07974, USA. [10]New Jersey Institute of Technology, Newark, NJ 07102, USA.

*To whom correspondence should be addressed. E-mail: tom.krimigis@jhuapl.edu